

# Highly sensitive setup for tunable wavelength hyper-Rayleigh scattering with parallel detection and calibration data for various solvents

Jochen Campo, Filip Desmet, Wim Wenseleers\* and Etienne Goovaerts

Department of Physics, University of Antwerp (campus Drie Eiken), Universiteitsplein 1, B-2610 Antwerpen, Belgium

\*Corresponding author: [Wim.Wenseleers@ua.ac.be](mailto:Wim.Wenseleers@ua.ac.be)

**Abstract:** A very sensitive experimental setup for accurate wavelength-dependent hyper-Rayleigh scattering (HRS) measurements of the molecular first hyperpolarizability  $\beta$  in the broad fundamental wavelength range of 600 to 1800 nm is presented. The setup makes use of a stable continuously tunable picosecond optical parametric amplifier with kilohertz repetition rate. To correct for multi-photon fluorescence, a small spectral range around the second harmonic wavelength is detected in parallel using a spectrograph coupled to an intensified charge-coupled device. Reliable calibration against the pure solvent is possible over the full accessible spectral range. An extensive set of wavelength-dependent HRS calibration data for a wide range of solvents is presented, and very accurate measurements of the  $\beta$  dispersion of the well-known nonlinear optical chromophore Disperse Red 1 are demonstrated.

© 2009 Optical Society of America

OCIS codes: (120.5820) Scattering measurements; (160.4890) Organic Materials; (300.6420) Spectroscopy, nonlinear; (160.4330) Nonlinear optical materials; (190.4710) Optical nonlinearities in organic materials.

---

## References and links

1. D. S. Chemla and J. Zyss, *Nonlinear Optical Properties of Organic Molecules and Crystals* (Academic Press, Orlando, 1987).
2. P. N. Prasad and D. J. Williams, *Introduction to Nonlinear Optical Effects in Molecules and Polymers* (New York, 1991).
3. R. W. Terhune, P. D. Maker, and C. M. Savage, "Measurements of nonlinear light scattering", *Phys. Rev. Lett.* **14**, 681-684 (1965).
4. K. Clays and A. Persoons, "Hyper-Rayleigh Scattering in Solution", *Phys. Rev. Lett.* **66**, 2980-2983 (1991).
5. J. Zyss and I. Ledoux, "Nonlinear Optics in Multipolar Media – Theory and Experiments", *Chem. Rev.* **94**, 77-105 (1994).
6. S. Stadler, F. Feiner, C. Brauchle, S. Brandl, and R. Gompper, "Determination of the first hyperpolarizability of four octupolar molecules and their dipolar subunits via hyper-Rayleigh scattering in solution", *Chem. Phys. Lett.* **245**, 292-296 (1995).
7. P. Kaatz and D. P. Shelton, "Polarized hyper-Rayleigh light scattering measurements of nonlinear optical chromophores", *J. Chem. Phys.* **105**, 3918-3929 (1996).
8. V. Ostroverkhov, R. G. Petschek, K. D. Singer, L. Sukhomlinova, R. J. Twieg, S. X. Wang, and L. C. Chien, "Measurements of the hyperpolarizability tensor by means of hyper-Rayleigh scattering", *J. Opt. Soc. Am. B-Opt. Phys.* **17**, 1531-1542 (2000).
9. C. H. Wang, J. N. Woodford, C. Zhang, and L. R. Dalton, "Resonant and nonresonant hyper-Rayleigh scattering of charge-transfer chromophores", *J. Appl. Phys.* **89**, 4209-4217 (2001).
10. L. C. T. Shoute, H. Y. Woo, D. Vak, G. C. Bazan, and A. M. Kelley, "Solvent effects on resonant first hyperpolarizabilities and Raman and hyper-Raman spectra of DANS and a water-soluble analog", *J. Chem. Phys.* **125**, 054506 (2006).
11. J. L. Oudar and D. S. Chemla, "Hyperpolarizabilities of Nitroanilines and Their Relations to Excited-State Dipole-Moment", *J. Chem. Phys.* **66**, 2664-2668 (1977).
12. S. Stadler, R. Dietrich, G. Bourhill, C. Brauchle, A. Pawlik, and W. Grahn, "First hyperpolarizability measurements via hyper-Rayleigh scattering at 1500 nm", *Chem. Phys. Lett.* **247**, 271-276 (1995).

13. M. A. Pauley and C. H. Wang, "Hyper-Rayleigh scattering measurements of nonlinear optical chromophores at 1907 nm", *Chem. Phys. Lett.* **280**, 544-550 (1997).
14. C. C. Hsu, S. Liu, C. C. Wang, and C. H. Wang, "Dispersion of the first hyperpolarizability of a strongly charge-transfer chromophore investigated by tunable wavelength hyper-Rayleigh scattering", *J. Chem. Phys.* **114**, 7103-7108 (2001).
15. A. M. Kelley, "Frequency-dependent first hyperpolarizabilities from linear absorption spectra", *J. Opt. Soc. Am. B-Opt. Phys.* **19**, 1890-1900 (2002).
16. A. M. Moran, D. S. Ego, M. Blanchard-Desce, and A. M. Kelley, "Vibronic effects on solvent dependent linear and nonlinear optical properties of push-pull chromophores: Julolidinmalononitrile", *J. Chem. Phys.* **116**, 2542-2555 (2002).
17. C. H. Wang, Y. C. Lin, O. Y. Tai, and A. K. Y. Jen, "Hyper-Rayleigh scattering and frequency dependence of the first molecular hyperpolarizability of a strong charge-transfer chromophore", *J. Chem. Phys.* **119**, 6237-6244 (2003).
18. O. Y. H. Tai, C. H. Wang, H. Ma, and A. K. Y. Jen, "Wavelength dependence of first molecular hyperpolarizability of a dendrimer in solution", *J. Chem. Phys.* **121**, 6086-6092 (2004).
19. S. T. Hung, C. H. Wang, and A. M. Kelley, "Resonant Raman spectra and first molecular hyperpolarizabilities of strongly charge-transfer molecules", *J. Chem. Phys.* **123**, (2005).
20. L. C. T. Shoute, G. P. Bartholomew, G. C. Bazan, and A. M. Kelley, "Resonance hyper-Raman excitation profiles of a donor-acceptor substituted distyrylbenzene: One-photon and two-photon states", *J. Chem. Phys.* **122**, (2005).
21. L. C. T. Shoute, M. Blanchard-Desce, and A. M. Kelley, "Resonance hyper-Raman excitation profiles and two-photon states of a donor-acceptor substituted polyene", *J. Phys. Chem. A* **109**, 10503-10511 (2005).
22. L. C. T. Shoute, R. Helburn, and A. M. Kelley, "Solvent effects on the resonance Raman and hyper-Raman spectra and first hyperpolarizability of N,N-dipropyl-p-nitroaniline", *J. Phys. Chem. A* **111**, 1251-1258 (2007).
23. W. Leng and A. M. Kelley, "Hyper-Rayleigh and hyper-Raman scatterings with intermediate and two-photon resonances", *J. Chem. Phys.* **127**, (2007).
24. B. F. Levine and C. G. Bethea, "2<sup>nd</sup> and 3<sup>rd</sup> Order Hyperpolarizabilities of Organic-Molecules", *J. Chem. Phys.* **63**, 2666-2682 (1975).
25. K. D. Singer and A. F. Garito, "Measurements of Molecular 2<sup>nd</sup> Order Optical Susceptibilities Using DC Induced 2<sup>nd</sup> Harmonic-Generation", *J. Chem. Phys.* **75**, 3572-3580 (1981).
26. M. Joffre, D. Yaron, R. J. Silbey, and J. Zyss, "2<sup>nd</sup>-Order Optical Nonlinearity in Octupolar Aromatic Systems", *J. Chem. Phys.* **97**, 5607-5615 (1992).
27. C. H. Wang, J. N. Woodford, and A. K. Y. Jen, "Measurements of the first hyperpolarizabilities of thiophene-based charge-transfer chromophores with hyper-Rayleigh scattering at 1064 and 1907 nm", *Chem. Phys.* **262**, 475-487 (2000).
28. J. N. Woodford, C. H. Wang, A. E. Asato, and R. S. H. Liu, "Hyper-Rayleigh scattering of azulenic donor-acceptor molecules at 1064 and 1907 nm", *J. Chem. Phys.* **111**, 4621-4628 (1999).
29. J. L. Oudar, "Optical Nonlinearities of Conjugated Molecules – Stilbene Derivatives and Highly Polar Aromatic-Compounds", *J. Chem. Phys.* **67**, 446-457 (1977).
30. A. Otomo, M. Jager, G. I. Stegeman, M. C. Flipse, and M. Diemeer, "Key trade-offs for second harmonic generation in poled polymers", *Appl. Phys. Lett.* **69**, 1991-1993 (1996).
31. G. Berkovic, G. Meshulam, and Z. Kotler, "Measurement and analysis of molecular hyperpolarizability in the two-photon resonance regime", *J. Chem. Phys.* **112**, 3997-4003 (2000).
32. J. Campo, W. Wenseleers, E. Goovaerts, M. Szablewski, and G. Cross, "Accurate Determination and Modeling of the Dispersion of the First Hyperpolarizability of an Efficient Zwitterionic Nonlinear Optical Chromophore by Tunable Wavelength Hyper-Rayleigh Scattering", *J. Phys. Chem. C* **112**, 287-296 (2008).
33. M. C. Flipse, R. Dejonge, R. H. Woudenberg, A. W. Marsman, C. A. Vanwalree, and L. W. Jenneskens, "The Determination of First Hyperpolarizabilities  $\beta$  Using Hyper-Rayleigh Scattering – a Caveat", *Chem. Phys. Lett.* **245**, 297-303 (1995).
34. O. F. J. Noordman and N. F. van Hulst, "Time-resolved hyper-Rayleigh scattering: Measuring first hyperpolarizabilities  $\beta$  of fluorescent molecules", *Chem. Phys. Lett.* **253**, 145-150 (1996).
35. S. Stadler, G. Bourhill, and C. Brauchle, "Problems associated with hyper-Rayleigh scattering as a means to determine the second-order polarizability of organic chromophores", *J. Phys. Chem.* **100**, 6927-6934 (1996).
36. I. D. Morrison, R. G. Denning, W. M. Laidlaw, and M. A. Stammers, "Measurement of first hyperpolarizabilities by hyper-Rayleigh scattering", *Rev. Sci. Instrum.* **67**, 1445-1453 (1996).
37. G. Olbrechts, R. Strobbe, K. Clays, and A. Persoons, "High-frequency demodulation of multi-photon fluorescence in hyper-Rayleigh scattering", *Rev. Sci. Instrum.* **69**, 2233-2241 (1998).
38. E. Goovaerts, W. Wenseleers, M. H. Garcia, and G. H. Cross, "Design and Characterization of Organic and Organometallic Molecules for Second Order Nonlinear Optics", in *Handbook of Advanced Electronic and Photonic Materials and Devices*, edited by H. S. Nalwa (Academic Press, 2001), Vol. 9, pp. 127-191.
39. M. P. Robalo, A. P. S. Teixeira, M. H. Garcia, M. F. M. da Piedade, M. T. Duarte, A. R. Dias, J. Campo, W. Wenseleers, and E. Goovaerts, "Synthesis, characterisation and molecular hyperpolarisabilities of pseudo-octahedral hydrido(nitrile)iron(II) complexes for nonlinear optics: X-ray structure of [Fe(H)(dppc)<sub>2</sub>(4-NCC<sub>6</sub>H<sub>4</sub>NO<sub>2</sub>)] [PF<sub>6</sub>]-CH<sub>2</sub>Cl<sub>2</sub>", *Eur. J. Inorg. Chem.*, 2175-2185 (2006).

40. W. Wenseleers, A. W. Gerbrandij, E. Goovaerts, M. H. Garcia, M. P. Robalo, P. J. Mendes, J. C. Rodrigues, and A. R. Dias, "Hyper-Rayleigh scattering study of  $\eta^5$ -monocyclopentadienyl-metal complexes for second order non-linear optical materials", *J. Mater. Chem.* **8**, 925-930 (1998).
41. K. Clays, "Molecular nonlinear optics: From para-nitroaniline to electrochemical switching of the hyperpolarizability", *J. Nonlinear Opt. Phys. Mater.* **12**, 475-494 (2003).
42. C. M. Savage and P. D. Maker, "Multichannel Photon Counting Spectrographic Detector System", *Appl. Opt.* **10**, 965 (1971).
43. M. J. French and D. A. Long, "Versatile Computer-Controlled Spectrometer for Hyper Rayleigh and Hyper Raman-Spectroscopy", *J. Raman Spectrosc.* **3**, 391-406 (1975).
44. V. N. Denisov, B. N. Mavrin, V. B. Podobedov, "Hyper-Raman scattering by vibrational excitations in crystals, glasses and liquids", *Phys. Rep.* **151**, 1-92 (1987).
45. P. Kaatz and D. P. Shelton, "Spectral measurements of hyper-Rayleigh light scattering", *Rev. Sci. Instrum.* **67**, 1438-1444 (1996).
46. P. Kaatz and D. P. Shelton, "Collision induced hyper-Rayleigh light scattering in  $\text{CCl}_4$ ", *Mol. Phys.* **88**, 683-691 (1996).
47. P. Kaatz and D. P. Shelton, "Spectral features of hyper-Rayleigh scattering in chloroform- $d^3$ ", *Opt. Commun.* **157**, 177-181 (1998).
48. C. J. F. Böttcher, *Dielectrics in Static Fields*. (Elsevier, Amsterdam, 1973).
49. M. Szablewski, P. R. Thomas, A. Thornton, D. Bloor, G. H. Cross, J. M. Cole, J. A. K. Howard, M. Malagoli, F. Meyers, J. L. Bredas, W. Wenseleers, and E. Goovaerts, "Highly dipolar, optically nonlinear adducts of tetracyano-*p*-quinodimethane: Synthesis, physical characterization, and theoretical aspects", *J. Am. Chem. Soc.* **119**, 3144-3154 (1997).
50. F. Kajzar, I. Ledoux, and J. Zyss, "Electric-field-induced optical second-harmonic generation in polydiacetylene solutions", *Phys. Rev. A: Gen. Phys.* **36**, 2210-2219 (1987).
51. Infrared absorption spectra of these and other organic solvents can be found, for instance, in the references mentioned in O. H. Wheeler, "Near Infrared Spectra of Organic Compounds", *Chem. Rev.* **59**, 629-666 (1959). Absorption spectra starting from 3000 nm can also be consulted online in the NIST Standard Reference Database <http://webbook.nist.gov/chemistry/>, (2005), where 8700 different compounds are listed.
52. W. Koban, J. D. Koch, R. K. Hanson, and C. Schulz, "Absorption and fluorescence of toluene vapor at elevated temperatures", *Phys. Chem. Chem. Phys.* **6**, 2940-2945 (2004).
53. J. R. Partington, *Physico-Chemical Optics*. (Longmans, London, 1967).
54. A. Samoc, "Dispersion of refractive properties of solvents: Chloroform, toluene, benzene, and carbon disulfide in ultraviolet, visible, and near-infrared", *J. Appl. Phys.* **94**, 6167-6174 (2003).
55. W. E. Forsythe, *Smithsonian Physical Tables*, 9 ed. (Smithsonian Institution, Washington, 1954, Table 551).
56. *International Critical Tables of Numerical Data, Physics, Chemistry and Technology*. (Maple Press Company, York, PA, 1930).
57. D. N. Nikogosyan, *Properties of Optical and Laser-Related Materials*. (John Wiley & Sons, Chichester, UK, 1997).
58. R. C. Weast, *CRC Handbook of Chemistry and Physics*. (CRC, Boca Raton, FL, 1980).
59. C. Marsden and S. Mann, *Solvents Guide*. (Clever-Hume, London, 1963).
60. *Chemist's Handbook*, edited by B. P. Nikolskii (Khimiya, Leningrad, 1965), Vol. 4.
61. R. E. Kagarise, "Infrared Dispersion of Some Organic Liquids", *J. Opt. Soc. Am.* **50**, 36-39 (1960).
62. J. R. Krivacic and D. W. Urry, "Ultraviolet and Visible Refractive Indices of Spectro-Quality Solvents", *Anal. Chem.* **42**, 596 (1970).
63. J. E. Bertie and Z. Lan, "The Refractive-Index of Colorless Liquids in the Visible and Infrared – Contributions from the Absorption of Infrared and Ultraviolet-Radiation and the Electronic Molar Polarizability Below  $20500\text{ cm}^{-1}$ ", *J. Chem. Phys.* **103**, 10152-10161 (1995).
64. *Concise Encyclopedia Chemistry*, edited by H.-D. Jakubke and H. Jeschkeit (Walter de Gruyter Berlin, New York, 1994).
65. J. Ans, E. Lax, and M. D. Lechner, *Taschenbuch für Chemiker und Physiker: Physikalisch-chemische Daten*. (Springer-Verlag Berlin Heidelberg, New York, 1992).
66. E. Moreels, C. Degreef, and R. Finsy, "Laser-Light Refractometer", *Appl. Opt.* **23**, 3010-3013 (1984).
67. A. F. Forziati, *J. Res. Natl. Bur. Stand.* **44**, 373 (1950).
68. J. Rheims, J. Koser, and T. Wriedt, "Refractive-index measurements in the near-IR using an Abbe refractometer", *Meas. Sci. Technol.* **8**, 601-605 (1997).
69. D. P. Seccombe, R. P. Tuckett, H. Baumgartel, and H. W. Jochims, "Vacuum-UV fluorescence spectroscopy of  $\text{CCl}_3\text{F}$ ,  $\text{CCl}_3\text{H}$  and  $\text{CCl}_3\text{Br}$  in the range 8–30 eV", *Phys. Chem. Chem. Phys.* **1**, 773-782 (1999).
70. M. Gocheldupuis, J. Delwiche, M. J. Hubinfranskin, J. E. Collin, F. Edard, and M. Tronc, "Electron-Energy Loss Spectroscopy of the Outer Valence Shells of Acetonitrile and Methyl Isocyanide", *J. Am. Chem. Soc.* **112**, 5425-5431 (1990).
71. J. M. Jung and H. Gress, "Single-photon absorption of liquid methanol and ethanol in the vacuum ultraviolet", *Chem. Phys. Lett.* **359**, 153-157 (2002).
72. H. Hayashi, N. Watanabe, Y. Udagawa, and C. C. Kao, "Optical spectra of liquid water in vacuum UV region by means of inelastic X-ray scattering spectroscopy", *J. Chem. Phys.* **108**, 823-825 (1998).

73. G. R. Burton, W. F. Chan, G. Cooper, and C. E. Brion, "Valence-Shell and Inner-Shell (Cl 2p, 2s, C 1s) Photoabsorption and Photoionization of Carbon-Tetrachloride – Absolute Oscillator-Strengths (5–400 eV) and Dipole-Induced Breakdown Pathways", *Chem. Phys.* **181**, 147-172 (1994).
74. B. Trost, J. Stutz, and U. Platt, "UV-absorption cross sections of a series of monocyclic aromatic compounds", *Atmos. Environ.* **31**, 3999-4008 (1997).
75. L. R. Dalton, A. Harper, A. Ren, F. Wang, G. Todorova, J. Chen, C. Zhang, and M. Lee, "Polymeric electro-optic modulators: From chromophore design to integration with semiconductor very large scale integration electronics and silica fiber optics", *Ind. Eng. Chem. Res.* **38**, 8-33 (1999).
76. S. Stadler, R. Dietrich, G. Bourhill, and C. Brauchle, "Long-wavelength first hyperpolarizability measurements by hyper-Rayleigh scattering", *Opt. Lett.* **21**, 251-253 (1996).
77. L. T. Cheng, W. Tam, S. H. Stevenson, G. R. Meredith, G. Rikken, and S. R. Marder, "Experimental Investigations of Organic Molecular Nonlinear Optical Polarizabilities 1. Methods and Results on Benzene and Stilbene Derivatives", *J. Phys. Chem.* **95**, 10631-10643 (1991).
78. M. Blanchard-Desce, J. B. Baudin, L. Jullien, R. Lorne, O. Ruel, S. Brasselet, and J. Zyss, "Towards highly efficient nonlinear optical chromophores: molecular engineering of octupolar molecules", *Opt. Mater.* **12**, 333-338 (1999).
79. S. F. Hubbard, R. G. Petschek, and K. D. Singer, "Spectral content and dispersion of hyper-Rayleigh scattering", *Opt. Lett.* **21**, 1774-1776 (1996).
80. S. R. Marder, L. T. Cheng, B. G. Tiemann, A. C. Friedli, M. Blanchard-Desce, J. W. Perry, and J. Skindhoj, "Large 1<sup>st</sup> Hyperpolarizabilities in Push-Pull Polyenes by Tuning of the Bond-Length Alternation and Aromaticity", *Science* **263**, 511-514 (1994).
81. S. R. Marder, C. B. Gorman, F. Meyers, J. W. Perry, G. Bourhill, J. L. Bredas, and B. M. Pierce, "A Unified Description of Linear and Nonlinear Polarization in Organic Polymethine Dyes", *Science* **265**, 632-635 (1994).
82. C. R. Mendonca, A. Dhanabalan, D. T. Balogh, L. Misoguti, D. S. dos Santos, M. A. Pereira-da-Silva, J. A. Giacometti, S. C. Zilio, and O. N. Oliveira, "Optically induced birefringence and surface relief gratings in composite Langmuir-Blodgett (LB) films of poly[4'-[[2-(methacryloyloxy)ethyl]ethylamino]-2-chloro-4-nitroazobenzene (HPDR13) and cadmium stearate", *Macromolecules* **32**, 1493-1499 (1999).

---

## 1. Introduction

Conjugated organic molecules are very promising building blocks for nonlinear optical (NLO) materials [1,2]. The high polarizability of their  $\pi$ -electron system leads to a large NLO response, which can be further optimized by chemical engineering. Other potential advantages of organic over inorganic materials are the relative ease of production (possibly at low cost) and their low dielectric constant resulting in a fast response time of electro-optic (EO) devices. At present, hyper-Rayleigh scattering (HRS) or second harmonic light scattering [3] is the main technique to measure the first hyperpolarizability  $\beta$  [4-10], which describes the second order NLO response at the molecular level. However, HRS measurements are usually performed at a single wavelength in the near infrared (NIR; *e.g.* 1064 nm using a Nd:YAG laser system), which, for typical NLO chromophores having an intramolecular charge-transfer (CT) transition in the visible region, results in  $\beta$  values that are strongly influenced by (two-photon) resonant enhancement. Because of this, the derivation of  $\beta$  at other wavelengths, and in particular the extrapolation to the static limit, is severely hampered. This complicates the comparison of  $\beta$  between different molecules and the assessment of their potential for EO applications. The simple two-level model (TLM) of Oudar and Chemla [11] is expected to be invalid in the resonance region because it does not consider any kind of line-broadening of the optical transitions. Despite this fact, it is almost universally applied in the literature to derive static  $\beta$  values from (nearly) resonant ones. To avoid the resonance effect on  $\beta$ , or at least to enter into a region where the use of the above undamped TLM becomes more acceptable, HRS measurements have been performed at a wavelength further in the infrared (IR). As a good example of this, Stadler *et al.* [12] were the first to perform HRS at 1500 nm, and later on Pauley and Wang [13] used the fundamental wavelength of 1907 nm accessible by Raman-shifting the Nd:YAG output in an H<sub>2</sub> cell. However, since typical efficient NLO chromophores exhibit a CT-transition far to the red (often extending well into the NIR), the second harmonic wavelength can still be quite close to resonance, even in case of very long fundamental wavelength. Also, once a reliable static value  $\beta_0$  is obtained, it is important for

applications to determine the (resonant) value for a specific NLO process at a given working wavelength (for instance,  $\beta$  for the EO effect at the telecommunication wavelengths of 1300 or 1500 nm). Because the wavelength-dependence of the first hyperpolarizability  $\beta$  is still not well-understood [10,14-23], it is necessary to determine this dispersion behavior experimentally by wavelength-dependent HRS measurements. The HRS technique is based on incoherent second harmonic generation (SHG) by the randomly oriented molecules in a liquid solution, and is by far more straightforward to interpret than the previously often applied electric-field induced second harmonic generation (EFISHG) technique [24,25], where the (necessarily dipolar) molecules are aligned by use of an externally applied static electric field. With HRS, no external field is required and therefore it is possible to measure hyperpolarizabilities from molecules having any structure (*i.e.* dipolar or octupolar [5,26]).

In pioneering papers by Wang and co-workers [14,17,19,27] and more recently also by Shoute *et al.* [10,20-22], the resonance effect on the first hyperpolarizability was observed by performing HRS measurements at a number of different wavelengths. However, these measurements are generally characterized by a very low signal-to-noise (S/N) ratio, which was attributed to the noise of the detector and to intensity fluctuations of the incoming laser pulses [19]. Moreover, because the signal from the pure solvent [28] (and in reference [14] even the one from *para*-nitroaniline (*p*NA)) could not be detected at longer wavelengths, two different reference standards (*p*NA and Disperse Red 1 (DR1)) had to be used for external calibration in different wavelength regions, almost inevitably leading to systematic errors as *a priori* the strong  $\beta$  dispersion of the reference standards themselves is unknown. The large scatter in their results makes it impossible to decide between the various possible  $\beta$  dispersion models [16,20,21,29-31], which often exhibit subtle differences in the resonance region with however strong effects on the static value  $\beta_0$  [32]. Hence, there is a strong need for detailed and accurate measurements of the  $\beta$  dispersion of organic molecules over a wide wavelength range around and beyond their absorption resonance. In this work we present a sensitive setup with parallel detection enabling wavelength-dependent HRS measurements with excellent S/N ratio and with reliable calibration against the pure solvent over a very broad wavelength range. Because the pure solvent exhibits only very limited and smooth  $\beta$  dispersion (which can moreover be accurately modeled, see below), this yields consistency between the hyperpolarizabilities obtained at different wavelengths. With the present setup,  $\beta$  can be determined very accurately in the extremely broad fundamental wavelength range of 600 to 1800 nm, uncovering in detail the molecular first hyperpolarizability dispersion.

## 2. Results

### 2.1 Experimental methods

The laser system (see Fig. 1) consists of a Ti:sapphire regenerative stretched-pulse amplifier (Spectra-Physics Spitfire with picosecond mask), seeded by a mode-locked Ti:sapphire laser (Spectra-Physics Tsunami, average power  $\sim 1$  W,  $\nu_{\text{rep}} = 82$  MHz, pulse duration  $\sim 100$  fs, wavelength: 800 nm) and optically pumped by a diode-pumped intracavity doubled Nd:YLF laser (Spectra-Physics Evolution, average power = 11 W,  $\nu_{\text{rep}} = 1.5$  kHz, pulse duration = 200 ns, wavelength: 527 nm). The Ti:sapphire laser is pumped in turn by means of an argon ion laser (Spectra-Physics BeamLok 2080, all lines) or a diode-pumped intracavity doubled Nd:YVO<sub>4</sub> laser (Spectra-Physics Millennia Pro *s*-Series, power  $\sim 7$  W, wavelength: 532 nm). The regenerative amplifier contains a spectral mask to yield amplified pulses with a 2 ps (instead of 100 fs) duration at the repetition rate  $\nu_{\text{rep}}$  of 1.5 kHz with an average power of about 800 mW. These pulses are used to pump an optical parametric amplifier (Spectra-Physics OPA-800CP), the output wavelength of which (of signal or idler beams or their 2<sup>nd</sup> or 4<sup>th</sup> harmonics) can be tuned from 300 nm to 3  $\mu\text{m}$ . The 2 ps pulses with correspondingly narrower spectral bandwidth allow for an excellent spectral discrimination between HRS and multi-photon fluorescence (see below) and at the same time yield a more optimal compromise

between HRS signal intensity and unwanted higher order effects, such as supercontinuum generation, which often occur with femtosecond pulses. In this work, we use the frequency-doubled signal beam in the range of 600 to 800 nm, the doubled idler beam from 800 to 1072 nm, the signal beam from 1072 nm to 1600 nm, and the idler beam from 1600 to 1800 nm. The pulse energy at the sample varies from 3–10  $\mu\text{J}$  below 1072 nm, over 10–40  $\mu\text{J}$  from 1072 to 1600 nm, to 10–15  $\mu\text{J}$  above 1600 nm. A small fraction ( $\sim 5\%$ ) of the laser power is split off and frequency-doubled by means of a BBO-crystal ( $\beta$ -barium borate,  $\beta$ -BaB<sub>2</sub>O<sub>4</sub>). The second harmonic is then separated from the fundamental beam by dichroic mirrors, and detected with a silicon PIN-diode. In this way, the HRS measurements can be corrected for (short term) fluctuations in pulse shape and laser power. However, it is found that when the laser power is quite stable, this procedure is not useful, and it is therefore not applied in most of the measurements presented here.

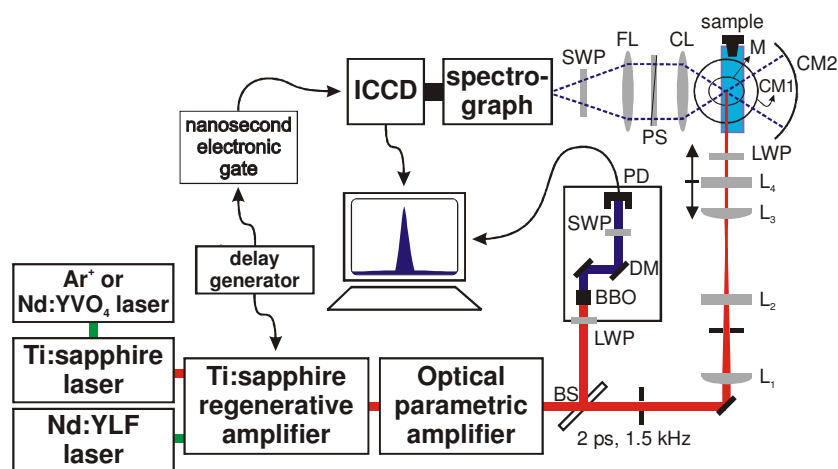


Fig. 1. Experimental setup for wavelength-dependent hyper-Rayleigh scattering measurements. **BS**: beamsplitter, **L(S)WP**: long (short) wavelength pass filter, **BBO**:  $\beta$ -barium borate frequency-doubling crystal, **DM**: dichroic mirror, **PD**: photodiode, **L<sub>1</sub>-L<sub>4</sub>**: cylindrical lenses, **M**: mirror, **CM1,2**: confocal mirrors, **CL**: collection lens, **PS**: polarization scrambler, **FL**: focusing lens.

After the appropriate filtering with long wave passing glass filters, the horizontal laser bundle is reflected upwards by mirror **M** and focused onto the sample, which consists of a dilute solution of the compound under study in a square fused silica cell (1 cm path length). The focus is positioned at half height in the horizontally oriented cell, just next to the cell wall closest to the collection lens **CL** (see below), to minimize reabsorption of the second harmonic light. To achieve a sufficiently high intensity while avoiding higher order effects such as self-(de)focusing and/or dielectric breakdown and at the same time limiting the intensity on the cell windows, the laser beam is focused only in one direction by means of cylindrical lenses **L<sub>1</sub>-L<sub>4</sub>**. Lenses **L<sub>1</sub>** and **L<sub>3</sub>** are forming a lens with large focal length, resulting in a narrow but to a good approximation parallel beam in one direction, whereas in the other direction the beam is tightly focused by lenses **L<sub>2</sub>** and **L<sub>4</sub>** which form a lens with short focal length. For  $\lambda = 1072$  nm, the dimensions of the laser beam (perpendicular to the propagation direction) at the focus are approximately 100  $\mu\text{m}$  in the focused and 1.5 mm in the collimated direction, as determined by means of a webcam with its lens and IR filter removed. The beam, traveling upwards through the sample, is then reflected downwards by use of a spherical confocal mirror (**CM1**) and thereby focused again on the sample close to but not overlapping with the upward beam. The generated hyper-Rayleigh light is collected at right angle by means of a photographic collection lens (**CL**,  $f = 50$  mm, up to  $f:1.4$ ) and imaged by an achromatic lens (**FL**,  $f = 100$  mm), through appropriate short wave pass filters, onto the

entrance slit of a spectrograph (ruled grating, 1180 grooves/mm, 500 nm blaze,  $f = 250$  mm), coupled to an intensified charge-coupled device (ICCD, Stanford Computer Optics, 4 Quik E) with nanosecond gating. In this way, parallel detection is obtained of a narrow spectral range ( $\sim 23$  nm) around the second harmonic wavelength, with single-photon sensitivity. The ICCD consists of a dual-stage microchannel plate image intensifier with an enhanced IR photocathode (sensitivity specified up to 900 nm), the intensified output of which (phosphor screen) is imaged onto a CCD using a lens. The CCD operates at room temperature and its analog video signal is digitized by a frame grabber board (25Hz). Frames are accumulated in software. In order to achieve single-photon sensitivity, even in long integrations (thousands of frames), a thresholding scheme is implemented in hardware simply by setting the signal voltage range of the input amplifier of the analog-to-digital converter: the lower signal level is set to a value (typically  $\sim 155$  mV) well above the dark noise of the CCD, but sufficiently low to register most actual (intensified) photon events, while the upper signal level is set as low as possible, corresponding to a maximum amplification. In this way, the dark noise (including read-out noise) of the CCD is completely eliminated and the S/N ratio in the limit of weak signals (few photons per frame) is improved by orders of magnitude. The only remaining source of dark noise is the actual dark electrons emitted by the photocathode. A (limited) further improvement in S/N ratio could be envisaged by combining the thresholding with single-photon counting in software. The sensitivity variation across the ICCD (mainly caused by vignetting by the lens between the phosphor screen and the CCD) is corrected based on a two-photon absorption induced fluorescence measurement of a dye with a broad fluorescence spectrum (for instance *p*-bis(*o*-methylstyryl)benzene (bisMSB)). To suppress stray light, dark-counts and cosmic rays, a 20 ns time gating is used, synchronized with the arrival of the laser pulses (using the output from the delay generator of the laser amplifier for triggering). If desired, the time window can be shortened down to 1 ns, for instance to suppress slow fluorescence contributions. However, for all our measurements a 20 ns time window worked well and puts less stringent requirements on timing accuracy (the time delay between the output of the amplifier and the trigger pulse of the detector needed no adjustment for years).

If no absorption of the second harmonic wavelength occurs (and hence no correction for reabsorption is necessary), a large spherical collection mirror (**CM2**, see Fig. 1) can be used to gather also the HRS light scattered in the opposite direction. The use of this extra mirror results in an increase of the signal by more than 50 %. A polarization scrambler is placed after the collection lens to eliminate the polarization dependence of the spectrograph. Due to the variation of the divergence of the OPA laser bundle and the refractive index dispersion of the cylindrical lens  $L_4$  which focuses this beam onto the sample, the (vertical) position of the focus needs to be reoptimized (*i.e.* centered in the cell) for every wavelength by shifting this focusing lens with a micrometer translation stage. Also for different solvents the focus position needs to be readjusted. The optimal position of the focusing lens as a function of wavelength and refractive index was determined (once) by means of two-photon fluorescence from concentrated solutions of different dyes for the different wavelength regions, yielding a focus visible to the naked eye. We used a polyphenylene-vinylene polymer (poly[2-methoxy-5-3(3',7'-dimethyloctyloxy)-1-4-phenylene vinylene, MDMO-PPV) above 1400 nm, rhodamine 6G from 700 to 1400 nm, fluorescein below 700 nm and bisMSB at 600 nm. Note that for this purpose, it is important to dissolve the dyes in the solvent which is used for the measurement, or at least in a solvent having approximately the same index of refraction.

To limit the effect of photo-induced decomposition in the laser focus, the molecules in this small region are constantly refreshed during the measurement by stirring the liquid just next to the vertical laser beam with a small stirring bar inside the cuvette (Rank Brothers Ltd., electronic stirrer model 300, up to 1100 rpm). The presence of significant (local) laser-induced decomposition can be excluded by checking that the HRS signal is independent of the stirrer speed. Of course, other essential checks for decomposition include the measurement of the absorption spectra of the samples before and after the HRS measurements, and

reproducibility of subsequent HRS measurements. For the measurements at the shortest wavelengths, the UV transparency of the collection and focusing lenses between the sample and the spectrograph was determined by means of a deuterium lamp and a miniature spectrometer (Ocean Optics HR2000). At second harmonic wavelengths below 380 nm, the photographic lens needs to be replaced by a single component lens, while below 320 nm fused silica singlet lenses are required for both collection and imaging of the HRS light onto the spectrometer entrance. The combination of the spectrograph and the ICCD was found to be sensitive down to 270 nm, and the HRS signal of N,N-dimethylformamide (DMF) could still be detected (however extremely weakly) at the 2<sup>nd</sup> harmonic wavelength of 290 nm.

The detection of the spectrum is essential, because it enables correction for any contribution of multi-photon absorption induced fluorescence (MPF, typically much broader than the spectrally narrow HRS line, see Fig. 2). Indeed, many second order NLO molecules

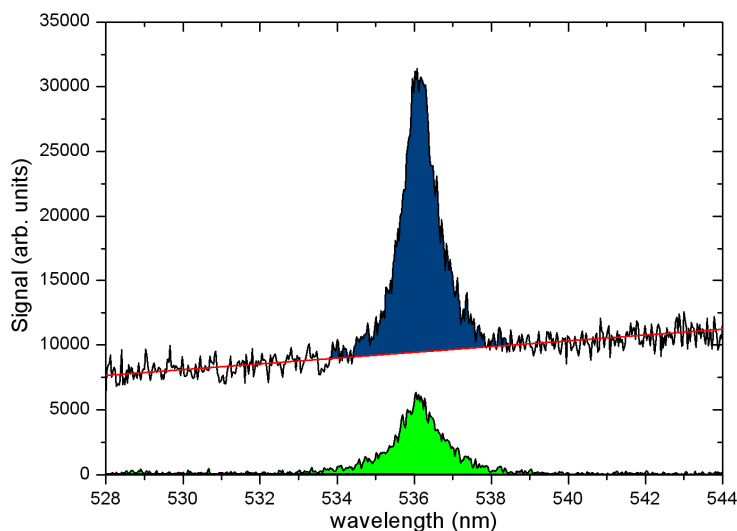


Fig. 2. Example of an HRS measurement (at the excitation wavelength of 1072 nm), clearly illustrating that correction for multi-photon fluorescence (red line) is needed. Blue: HRS signal of the solution, green: reference signal of the pure solvent.

exhibit significant two-photon fluorescence near the second harmonic wavelength and hence correction for this effect is required to obtain reliable first hyperpolarizabilities  $\beta$  [33-35]. Another method to suppress MPF has been developed by Noordman and van Hulst [34]. By detecting the *quasi*-instantaneous HRS light with a high time resolution of about 80 ps, they suppress the luminescence which is mostly occurring on nanosecond time scales. Several variants to this approach have been developed [36], including a method based on phase-sensitive detection [37]. However, this technique requires the measurements to be repeated at multiple demodulation frequencies (involving a complicated electronic detection scheme), followed by potentially very unreliable extrapolation to infinite frequency. Moreover, as correctly pointed out in reference [34], fluorescence signals are likely to contain much faster components (even shorter than 1 ps), which can not be excluded by electronic means. Hence, although the time-resolved techniques could be useful as an additional method to suppress MPF, the registration of a spectral range as is done in this work remains crucial to eliminate it reliably [32,36,38-40]. The only mentioned drawback of this wavelength-dependent method to correct for fluorescence is that it would be time consuming [41]. This however is not the case here, as the entire spectral range of interest is detected in parallel. Quite remarkably, a hyper-Rayleigh and hyper-Raman scattering setup at a single wavelength (694 nm, from a ruby laser), with multi-channel detection to speed up the measurements, has been reported already

in 1971 [42], and hyper-Rayleigh and hyper-Raman scattering for water, chloroform and carbon tetrachloride was later effectively demonstrated using such a system [43,44]. However, such techniques are not used in more recent HRS work, which often (without obvious reason) even omits the spectral analysis of the scattered light altogether. The setup described here is the first to combine a sensitive parallel detection with a modern, tunable laser system.

In a typical HRS measurement, ICCD images are recorded alternatingly for the solution and the pure reference solvent. These images are integrated vertically (*i.e.* parallel with the entrance slit of the spectrograph), which, after sensitivity correction, yields spectra such as shown in Fig. 2. The outer parts of the spectra can now be used to determine and subtract the MPF background (usually by means of a linear fit), so that only the genuine HRS signal remains. It is important to note that the HRS from small solvent molecules (*e.g.* chloroform) has a significant spectral width, with broad tails due to fast molecular rotation and collisions [45-47]. Therefore, care must be taken to choose a sufficiently wide central interval over which the HRS signal is integrated. In most of our measurements, we used an integration window of about 200 cm<sup>-1</sup> (increasing at shorter wavelengths up to 350 cm<sup>-1</sup> to account for spectral resolution), as clipping the tails beyond this window results in errors less than 0.5 % for chloroform and most other solvents. Among the solvents studied here (see below), only acetone and methanol display even wider HRS signals. In these two cases, we used a broader interval of about 300 cm<sup>-1</sup> to keep the error below 2 %. On the other hand, the integration range should not be taken excessively wide, in order to avoid significant contributions from hyper-Raman scattering (*e.g.* among the solvents examined in this work, the lowest frequency significant hyper-Raman peak occurs in chloroform at about 760 cm<sup>-1</sup>, with an integrated intensity of about one third of that of the HRS itself).

In case of a dilute solution, equal refractive indices can be assumed for the solution and the pure solvent, so that identical refraction and reflection at the walls of the sample cell takes place. If furthermore spherical local field factors are used [48], the local field corrections also cancel in the expressions (unlike in EFISHG, this is usually a good approximation in HRS, even for relatively elongated chromophores [49]). The following expressions are obtained for the HRS signals of the pure solvent and the dilute solution respectively [4,35,38]:

$$S_{\text{solvent}}^{(2\omega)} \propto N_{\text{solvent}} \langle \beta_{\text{solvent}}^2 \rangle (P^{(\omega)})^2 \quad (1)$$

$$S_{\text{solution}}^{(2\omega)} \propto \left( N_{\text{solvent}} \langle \beta_{\text{solvent}}^2 \rangle + N_{\text{solute}} \langle \beta_{\text{solute}}^2 \rangle \right) (P^{(\omega)})^2. \quad (2)$$

In these expressions  $N$  is the number density,  $P^{(\omega)}$  is the power of the laser beam and  $\langle \beta^2 \rangle$  stands for the orientational average of the quadratic form of the  $\beta$  tensor component(s), which is observed in the incoherent HRS process. For unpolarized measurements with an incident laser beam linearly polarized along the laboratory  $Z$ -axis (as performed in this work),  $\langle \beta^2 \rangle$  is given by  $\langle \|\beta_{xxx}\|^2 \rangle + \langle \|\beta_{zzz}\|^2 \rangle$ . For a dilute solution, the density of the solvent molecules can again be assumed equal for the pure solvent and the solution, so that Eqs. (1) and (2) can be combined, yielding for the hyperpolarizability of the solute:

$$\langle \beta_{\text{solute}}^2 \rangle = \frac{N_{\text{solvent}}}{N_{\text{solute}}} \frac{S_{\text{solution}}^{(2\omega)} - S_{\text{solvent}}^{(2\omega)}}{S_{\text{solvent}}^{(2\omega)}} \langle \beta_{\text{solvent}}^2 \rangle. \quad (3)$$

If  $\beta_{zzz}$  (along the molecular  $z$ -axis) is assumed to be the only significant  $\beta$  component, the orientational average squared of the  $\beta$  tensor components is reduced to:

$$\langle \beta^2 \rangle = \langle \|\beta_{xzz}\|^2 \rangle + \langle \|\beta_{zzz}\|^2 \rangle = \frac{6}{35} \beta_{zzz}^2. \quad (4)$$

If this assumption is made for both the pure solvent and the solute molecules, Eq. (3) can be rewritten directly in terms of  $\beta_{zzz}$ :

$$\beta_{zzz}^{eff, solute} = \sqrt{\frac{N_{solvent}}{N_{solute}} \frac{S_{solution}^{(2\omega)} - S_{solvent}^{(2\omega)}}{S_{solvent}^{(2\omega)}}} \beta_{zzz}^{eff, solvent}. \quad (5)$$

This expression is applied in this work for the calculation of the  $\beta$  values. The assumption of a single dominant  $\beta$  component is usually valid for push-pull NLO chromophores (with the  $z$ -axis along the conjugated chain), but not for the pure solvent molecules. However, if the solvent is only used as a calibration standard for (unpolarized) HRS measurements on linear push-pull chromophores, it may still be convenient to express the solvent hyperpolarizability as an effective  $\beta_{zzz}$  for HRS, to be used in Eq. (5). Alternatively, one might use the actually

observed quantity  $\beta_{HRS} = \sqrt{\langle \|\beta_{xzz}\|^2 \rangle + \langle \|\beta_{zzz}\|^2 \rangle} = \sqrt{6/35} \beta_{zzz}^{eff}$ . Even in that case one

should keep in mind that these values merely represent effective hyperpolarizabilities for calibration of HRS and should not be physically interpreted as the hyperpolarizability of individual solvent molecules, because, unlike HRS from chromophores in dilute solution, HRS from a pure solvent is strongly influenced by short range orientational correlations and interactions between neighboring molecules [45-47]. All these effects are included in the *effective*  $\beta$  values for solvents used here.

Whenever the solvent hyperpolarizability is unknown, or the HRS signal of the pure solvent cannot be detected, it is necessary to compare signals of different solvents. In this case, the different degree of focusing of the incident laser beam and the different collection geometry of the HRS light, as well as the different local field factors need to be taken into account. For a Gaussian laser beam tightly focused in at least one direction inside a square sample cell, the solvent signal is given by [38]:

$$S_{solvent}^{(2\omega)} \propto n_{\omega} \frac{1}{n_{2\omega}^2} T_{\omega}^2 T_{2\omega} f_{\omega}^4 f_{2\omega}^2 N \langle \beta_{solvent}^2 \rangle (P_Z^{(\omega)})^2, \quad (6)$$

with  $T_{\omega}$  and  $T_{2\omega}$  the changes of the transmission factors (which can often be neglected) and  $f_{\omega}$  and  $f_{2\omega}$  the local field factors. For solvents in optical fields, spherical (Lorentz-Lorenz) local field factors are appropriate, given by [48]:

$$f_{\omega} = \frac{\varepsilon_{\omega} + 2}{3}, \quad (7)$$

with  $\varepsilon_{\omega}$  the dielectric constant. Eq. (6) will be applied below in the analysis of the HRS measurements in different solvents.

## 2.2 Selection and calibration of solvents

Many different criteria have to be considered in the choice of the solvent for wavelength-dependent HRS measurements. At the shortest wavelengths one needs sufficient UV transparency to avoid absorption of the generated second harmonic light, whereas at the long wavelength side it is essential that the solvent is sufficiently IR transparent to prevent absorption of the incident laser light. Furthermore, to enable precise calibration against the pure solvent, a strong HRS signal is usually preferable, although a weak solvent signal is

sometimes preferred for the measurement of solutes with low hyperpolarizabilities. Finally, also the stability and the solubility of the molecules under study influences the choice of an appropriate solvent. Therefore, in this work a wide range of solvents is selected and calibrated for tunable wavelength HRS, to allow consistent datasets to be obtained from measurements on molecules in different solvents and at different wavelengths. As a primary calibration standard for our measurements, we selected the effective value  $\beta_{zzz}^{eff} = 0.49 \times 10^{-30}$  esu for chloroform at 1064 nm from reference [50]. Although the use of this value neglects the off-diagonal tensor components and intermolecular interactions which are known to occur in chloroform [47], it is very often used, directly or indirectly, in literature to calibrate HRS data. Its use is further justified by the fact that it yields reasonable values for relatively well-known chromophores such as *p*NA (see reference [38] for a detailed discussion). However, very few absolute reference standards exist for NLO measurements, and a new, independent absolute standard would be highly desirable. If a more accurate absolute HRS standard would become available in the future, this would merely result in an overall scaling of the wavelength dependent calibration data obtained here, and would not affect the relative values between different solvents or wavelengths.

The IR transparency of organic solvents is often very poor due to the absorption bands associated with overtones and combination peaks involving C–H stretch vibrations. The absorption of an extensive series of solvents for use in NLO experiments in the NIR was determined with a Varian Cary 5 UV-Vis-NIR absorption spectrophotometer and is shown in Fig. 3. All solvents were measured as received from commercial suppliers without further purification [51]. From Fig. 3 it is clear that, for instance, HRS measurements at a fundamental wavelength longer than 1400 nm are not possible in methanol, and long-wavelength measurements in water are even more problematic. Chloroform on the other hand is a very interesting solvent for HRS, not only because it is very often used as a calibration standard, but also because it offers good transparency in the IR, having only a few narrow peaks arising from the single hydrogen atom in its chemical structure. With the continuously tunable laser system, these peaks can be easily avoided in a wavelength dependent HRS scan. The long-wavelength limit for HRS measurements in chloroform lies at about 1660 nm, at the very edge of the absorption peak at ~1690 nm. Furthermore, at the long wavelength side (> 1600 nm), both scattering efficiency and detector sensitivity decrease, so that measurements become more difficult and time consuming. To enable measurements at longer wavelengths without losing the feature of calibration against the pure solvent, we have looked for IR transparent solvents (ideally this means no hydrogens in the chemical structure) that exhibit also a strong HRS signal. Bromoform (Acros, 99 %, spectroscopic grade, stabilized) is found to be a promising candidate, having a more than six times stronger HRS signal than chloroform and very similar IR transparency. We also tried extremely IR transparent fluorinated and chlorinated solvents, such as carbon tetrachloride (Fluka, for HPLC,  $\geq 99.8$  % [GC]), perfluorohexane (Aldrich, 99 %), trichloroacetonitrile (Acros, 98 %), bromotrichloromethane (Acros, 99 %), chloropentafluorobenzene (Acros, 99 %) and hexachloroacetone (Acros, 99+ %), but unfortunately they all exhibit a relatively weak HRS signal (the actual signals before correction for the different refractive indices and local fields are about 1.38, 0.03, 0.96, 2.61, 1.01 and 1.64 times the chloroform signal respectively). Note however that the less common solvents are usually not commercially available in the highest purity grades (analytical/spectroscopic grade), and can therefore contain impurities which might interact with the dissolved molecules or cause decomposition. Also the UV transparency of these solvents is often very poor (*e.g.* *d*-DMF from Acros), which sometimes excludes their use at short wavelengths. Better IR transparency can also be obtained by using deuterated solvents (compare for example the absorption spectra of DMF and *d*-DMF in Fig. 3), being for

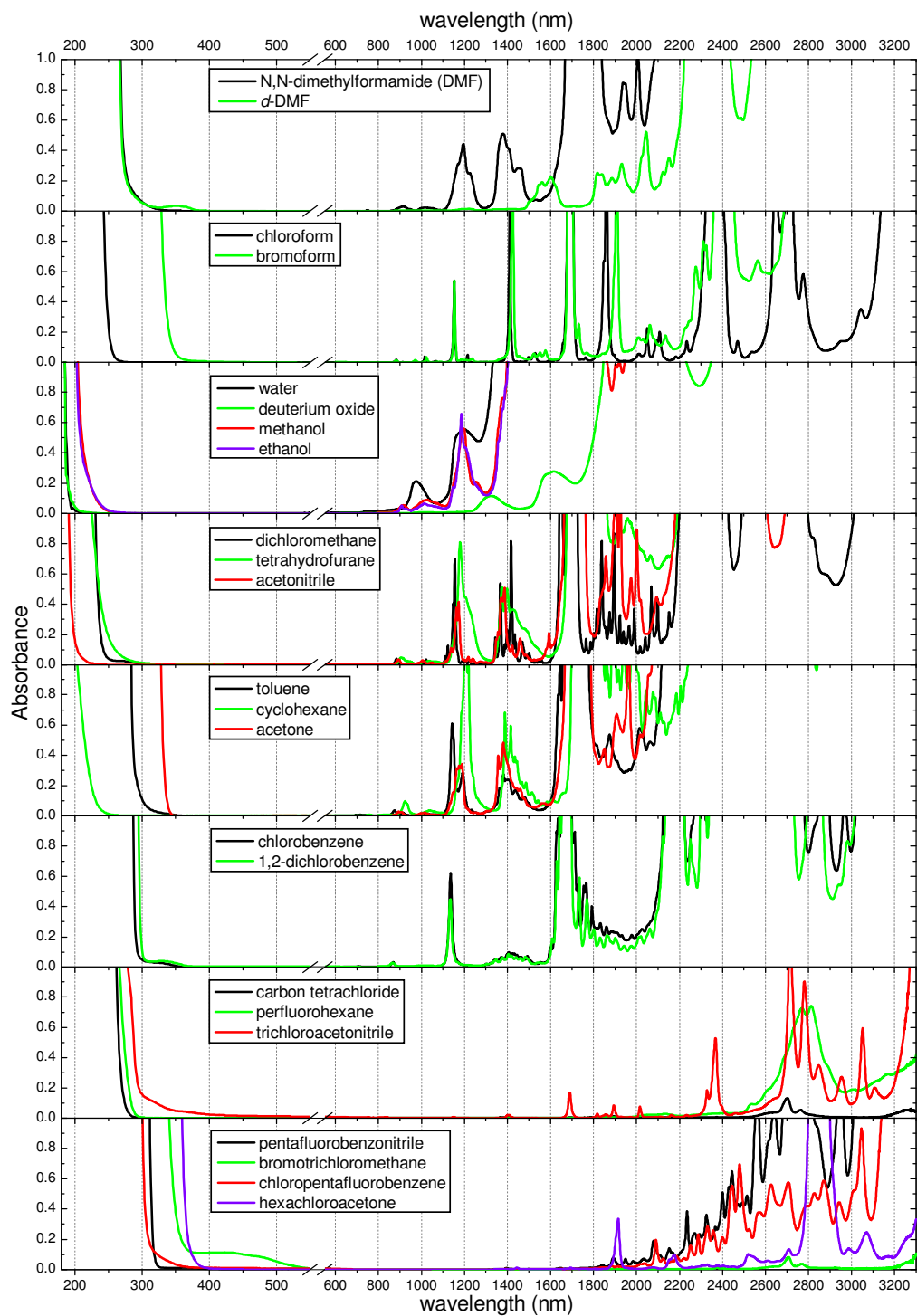


Fig. 3. UV-VIS-NIR absorption spectra of various solvents (1 cm path length), measured as received from commercial sources (see text).

this purpose electronically equivalent. The remaining specifications of the solvents shown in Fig. 3 (and used for the relative HRS measurements below) are: DMF (Acros, 99.8 %, for analysis ACS), *d*-DMF (Acros, 99.5 atom % D), chloroform (Acros, stabilized, spectrophotometric grade 99+ %), water (Milli-Q), D<sub>2</sub>O (Aldrich, 99.9 atom % D [glass distilled]), methanol (Vel, max 0.05 % water), ethanol (VWR, normapur, 96 %), dichloromethane (Aldrich, biotech grade, 99.9 %), tetrahydrofuran (Acros, 99.5 %, for spectroscopy), acetonitrile (Vel, for UV-IR spectroscopy), toluene (UCB, max. 0.0005 % thiophene), cyclohexane (Acros, spectrophotometric grade, 99+ %), acetone (Aldrich, 99.9+ %, HPLC Grade), chlorobenzene (Fisher Scientific, 99.99 % [GC]) and 1,2-dichlorobenzene (ACROS, spectrophotometric grade, 99+ %).

Two solvents were found to be particularly useful at long wavelengths: bromoform and pentafluorobenzonitrile (the latter possesses a more than 14 times stronger HRS signal compared to chloroform and a nearly perfect transparency in the IR region of interest). The latter solvent remained useful up to 1800 nm, only limited by the ~900 nm sensitivity cut-off of the ICCD camera (at 920 nm the HRS signal of the solvent became extremely weak). It should be noted that commercially available pentafluorobenzonitrile (from various suppliers) often exhibits very poor UV transparency (faintly yellow liquid) and often contains a lot of dust particles. Four batches were considered (Acros, 97 %; Aldrich, 99 %; Alfa Aesar, 98 %; Merck, for synthesis), and it was found that the one from Acros (absorption spectrum shown in Fig. 3) exhibits by far the best UV transparency and is therefore preferable for HRS. However, the Aldrich batch, despite its lower transparency at short wavelengths, yielded the same HRS signal within experimental error, provided that it was filtered (Gelman Sciences, 0.5  $\mu$ m, PTFE) before use to drastically reduce a fluctuating background from solid impurities.

In general, the dispersion of the first hyperpolarizability of the pure solvent is expected to have only very limited influence on HRS measurements, since they are practically always performed far from the UV transitions. However, for extensive wavelength-dependent measurements such as performed here on DR1 (see below) and in reference [32], this effect can become important. To determine the significance of this effect and to be able to correct for it, the  $\beta$  dispersion of eight different solvents (DMF, acetonitrile, methanol, water, acetone, toluene, carbon tetrachloride and pentafluorobenzonitrile) was examined by performing relative HRS measurements against chloroform (see Fig. 4). Due to the very poor IR transparency of water, accurate measurements for this solvent are only possible until 1072 nm, but a crude estimate of  $\beta$  could still be obtained at 1250 nm after major correction for fundamental absorption. The short wavelength limit for the measurements on toluene is imposed by very strong multi-photon fluorescence (linear fluorescence had indeed been observed for toluene at these short wavelengths [52]). The experimental error on the  $\beta$  values (not including the error on the primary reference standard chloroform) is varying from  $\pm 5$  % to  $\pm 10$  %, generally increasing towards shorter wavelengths where the signals decrease due to the combination of lower laser power, lower detection efficiency and less efficient collection by the UV lenses (compared to the achromatic lenses).

It is important to check whether no anomalies are found in the obtained dispersion curves near to the vibrational absorption bands of the solvents (C–H stretch overtones and combinations), either intrinsically through vibrational resonance contributions to  $\beta$  or through thermal lensing of the laser beam. This is excluded by the smooth dispersion observed for all of the solvents studied here. For instance both DMF and methanol are already absorbing at 1250 nm but the obtained  $\beta$  values still follow a smooth curve, well modeled with a simple TLM. In addition, the absence of such effects has also been demonstrated by comparing measurements on a zwitterionic chromophore in DMF and *d*-DMF [32]. The insensitivity of the present setup to thermal lensing effects (even in IR absorption bands with an absorbance of about 0.5 in a 1 cm path length cell) is ascribed to the combination used here of short

pulses and weak focusing. In contrast, thermal lensing effects have been reported [45] even at 1064 nm when using very tight focusing with 150 ns pulses.

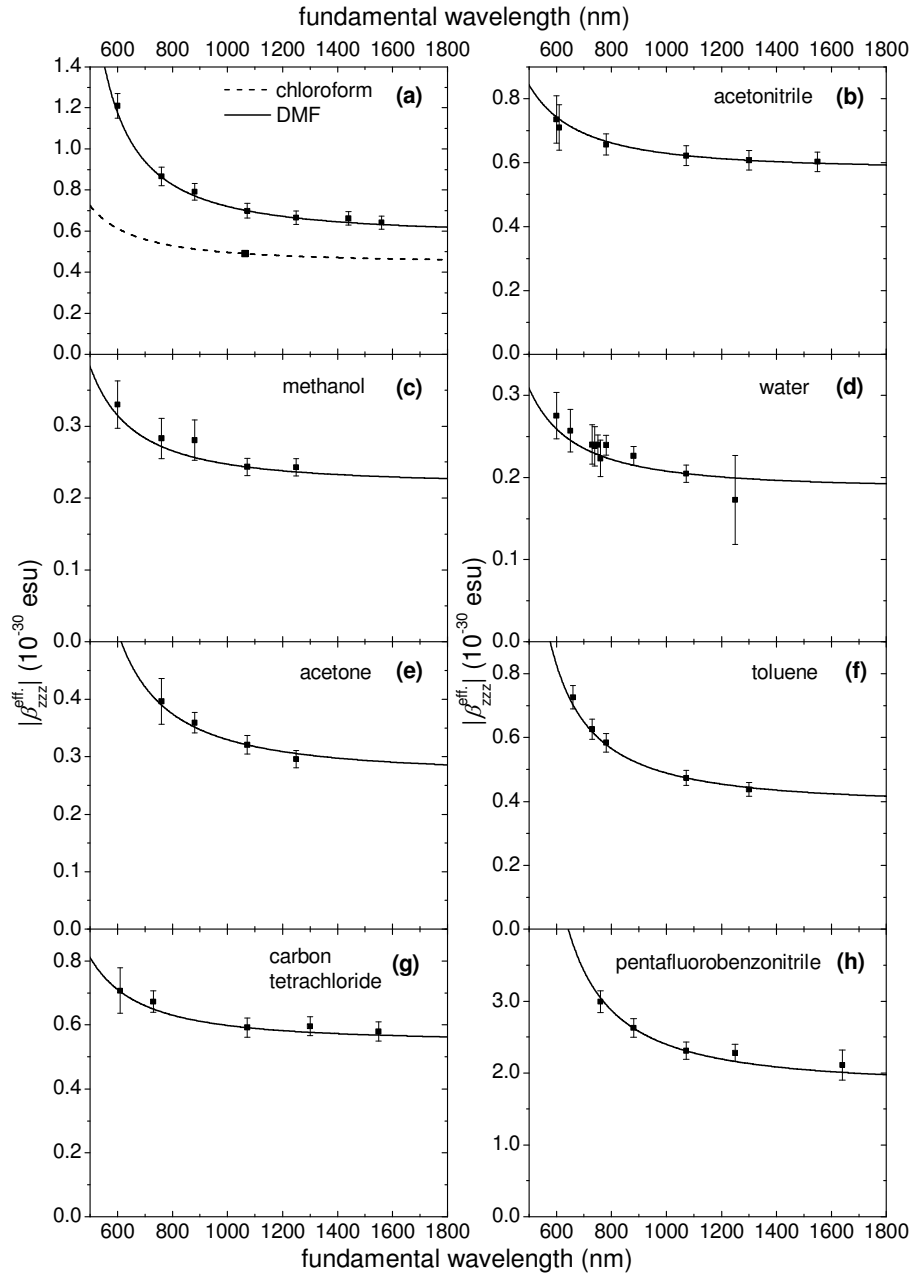


Fig. 4. HRS measurements of eight different solvents calibrated against chloroform. The  $\beta$  dispersion of chloroform itself is estimated using the undamped two-level model (dashed line in Fig. (a)). Symbols: experimental HRS data (except for chloroform, for which the calibration value is shown), lines: undamped two-level models (see Table 2 for the used  $\lambda_{\text{eg}}$  values).

To simplify the interpretation of these relative measurements, the spherical top mirror (CM1, see Fig. 1) as well as the spherical collection mirror (CM2) were not used during the experiments and the focus position was optimized for every particular solvent/wavelength combination. The refractive indices of the various solvents are needed to take into account the

different focusing of the laser beam, the different collection of the scattered light and the local field factors (see above). For all solvents except pentafluorobenzonitrile, the wavelength-dependence of the refractive index was extrapolated (interpolated for chloroform) by means of the Sellmeier dispersion formula [53] including only the first term, fitted to the experimental refractive indices at several wavelengths reported in the literature (see Table 1). No refractive index dispersion data could be found in the literature for pentafluorobenzonitrile, and hence a constant index was used ( $n = 1.4425$  at 589.3 nm [D line of Na] as obtained from the supplier). Note that Samoc [54] performed an extensive study concerning the dispersion of the refractive properties of several pure solvents (including chloroform), having the analysis of NLO measurements in mind. There it was stressed that, instead of the one-term Sellmeier formula, it is necessary to apply the Cauchy dispersion formula including three wavelength-dependent terms to correctly describe the refractive index dispersion. However, for some of the solvents studied here only a limited amount of literature data is available (*e.g.* only four data points in the range of 434–656 nm for dimethylformamide), which causes the Cauchy equation to give unrealistic results outside of the experimentally covered range. Because within this range, the deviations between the two formulas are small ( $< 1\%$ ), the Sellmeier formula including only the first term is selected in this work for the extrapolation of the refractive index dispersion of the pure solvents.

Table 1. Parameters used in the one-term Sellmeier expression [ $n(\lambda)^2 = 1 + A_1\lambda^2/(\lambda^2 - \lambda_1^2)$ ] to describe the refractive index dispersion of the pure solvents studied here. The references mentioned in the last column contain the experimental data to which the expression is fitted.

solvent	$\lambda_1$ (nm)	$A_1$	ref.
chloroform	107.933	1.054	[53,55-61]
DMF	117.456	1.002	[56]
acetonitrile	100.145	0.787	[56,62]
methanol	101.002	0.742	[55,56,63]
water	102.562	0.749	[55,56,62-65]
acetone	108.065	0.817	[55,56,63,66]
toluene	137.888	1.173	[53,55,57,66-68]
carbon tetrachloride	109.801	1.094	[55,64,66]

For some of the relative HRS measurements, one or both of the pure solvents exhibit optical absorption at the fundamental wavelength (see Fig. 3), for which hence a correction needs to be applied. Because HRS is proportional to the laser intensity squared, the hyper-Rayleigh scattered light can be considered to a good approximation to originate only from the laser focus at half height in the quartz cell. If  $A$  is the absorbance at the fundamental wavelength (1 cm path length), the intensity at this position will be attenuated by a factor  $10^{-A/2}$ , leading to the correction factor of  $10^A$  for the HRS signal.

The  $\beta$  dispersion of chloroform is estimated by means of the undamped two-level model (TLM) of Oudar and Chemla [11], taking the maximum of the longest wavelength absorption band of chloroform (143 nm [69]) as  $\lambda_{eg}$ , and  $0.49 \times 10^{-30}$  esu (EFISHG value from reference [50]) as  $\beta_{zzz}^{eff}$  value at 1064 nm (using the usual assumptions [38], see above). Although this strongly simplified model does not consider any kind of line-broadening of the optical transition, it is expected to give a good description for chloroform in the visible and IR region, far enough from the UV transition. The curves in Fig. 4 show the  $\beta$  dispersion of the examined solvents derived from the undamped TLM, with the static hyperpolarizability  $\beta_0$  adjusted to fit the experimental  $\beta$  values at 1072 nm. The used  $\lambda_{eg}$  and  $\beta_0$  values are summarized in Table 2.

Table 2. Parameters of the undamped TLM for the various solvents, corresponding to the curves in Fig. 4: the UV transition wavelength  $\lambda_{eg}$ , the effective static first hyperpolarizability  $\beta_{zzz,0}^{eff}$ , and the orientational average  $\langle \beta_0^2 \rangle = \langle \|\beta_{xxx,0}\|^2 \rangle + \langle \|\beta_{zzz,0}\|^2 \rangle$  multiplied with the number density of the solvent (as a measure for the HRS signal).

solvent	$\lambda_{eg}$ (nm)	$\beta_{zzz,0}^{eff}$ ( $10^{-30}$ esu)	$\langle \beta_0^2 \rangle \cdot N$ ( $10^{-60}$ esu·M)
chloroform	143 <sup>a</sup>	0.446	0.424
DMF	200 <sup>b</sup>	0.592	0.780
acetonitrile	129 <sup>c</sup>	0.578	1.097
methanol	152 <sup>d</sup>	0.219	0.203
water	146 <sup>c</sup>	0.186	0.329
acetone	194 <sup>b</sup>	0.270	0.170
toluene	205 <sup>b</sup>	0.390	0.245
carbon tetrachloride	131 <sup>f</sup>	0.548	0.532
pentafluorobenzonitrile	223 <sup>b</sup>	1.825	4.526

<sup>a</sup>ref. [69], <sup>b</sup>from vapor-phase absorption (see Fig. 5), <sup>c</sup>ref. [70], <sup>d</sup>ref. [71], <sup>e</sup>ref. [72], <sup>f</sup>ref. [73].

Because no (or not sufficient) vacuum UV data could be found in the literature for DMF, acetone, toluene and pentafluorobenzonitrile, we performed vapor-phase optical absorption measurements (see Fig. 5).

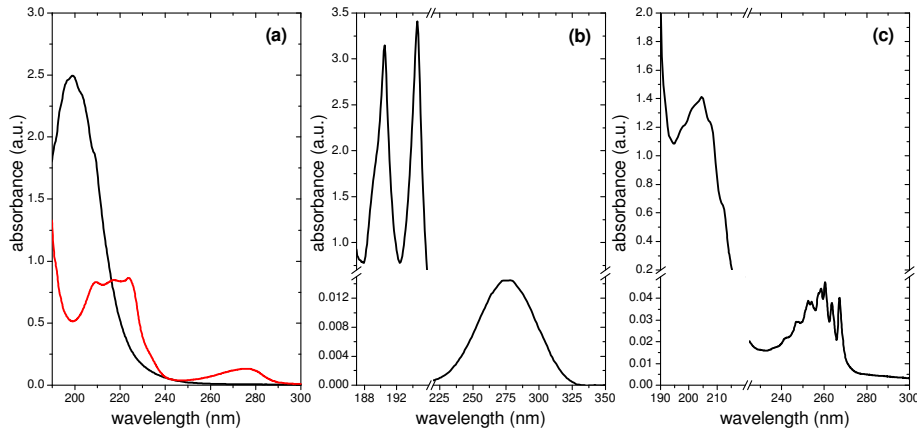


Fig. 5. Vapor-phase UV absorption of various solvents. (a) DMF (black curve) and pentafluorobenzonitrile (red curve), (b) acetone and (c) toluene.

Generally, the first *strong* UV transition is selected to determine  $\lambda_{eg}$ . It was indeed found that in many cases where the lowest energy transition is very weak, the  $\beta$  dispersion would be overestimated if the maximum of this weak band was adopted as  $\lambda_{eg}$ . For instance, in Fig. 5(a) it is seen that pentafluorobenzonitrile shows another UV transition at about 275 nm, more than five times weaker than the one at 223 nm which is used for the undamped TLM in Fig. 4. If this 275 nm transition is used instead, no acceptable agreement with the experimental data could be obtained, so indeed this lower energy transition is not giving a dominant contribution to  $\beta$ . The same is found to be true for the 276 nm transition observed in acetone, which is more than 250 times weaker than the selected 194 nm transition (see Fig. 5(b)), and for the highly resolved absorption band around 260 nm in toluene [74], which is about 30 times weaker than the chosen 205 nm transition (see Fig. 5(c)). In fact only for DMF (see Fig. 5(a))

and methanol [71] there was no need for such an approach, and the intense lowest absorption transition was selected for the TLM. While the selection of a single  $\lambda_{eg}$  for each solvent may seem somewhat arbitrary at first, the excellent consistency obtained with the extensive HRS data set for nine different solvents demonstrates the reliability of the calibration data (see Fig. 4), and the appropriateness of the undamped TLM for these solvents.

## 2.2 Application to the nonlinear optical dye Disperse Red 1

To demonstrate the qualities of the setup described in the previous section, we make use of the well-known organic dye molecule Disperse Red 1 (DR1, Fluka, analytical standard,  $\geq 96.0\%$ , for HPLC). DR1 is a classical donor-acceptor system with an azostilbene-derived structure, which belonged for a long time to the best nonlinear optical molecules [75], and which is still one of the most commonly used chromophores for fabricating NLO materials. Currently, DR1 is also very often used as an external reference standard for HRS [9,13,14,18,76]. Although both EFISHG and HRS measurements at a single wavelength have been performed on DR1 [77,78], the dispersion of its first hyperpolarizability has never been examined. An attempt to do so was reported in 1996 [79], but only two data points far from resonance could be obtained because close to resonance the HRS signal could not be distinguished from the broad two-photon fluorescence background. Our experimental HRS data for the DR1 molecule in the range of 600 to 1800 nm are shown in Fig. 6, together with the absorption spectrum in chloroform solution.

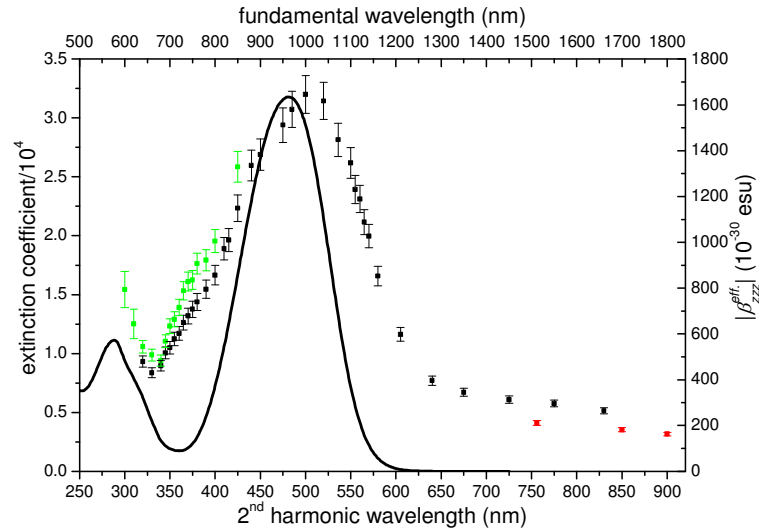


Fig. 6. Experimental HRS data obtained for Disperse Red 1 (DR1) in chloroform (black squares), acetonitrile (at shorter wavelengths, green squares) and pentafluorobenzonitrile (at longer wavelengths, red squares), corrected for the  $\beta$  dispersion of the pure solvents, and shown together with the UV-VIS absorption spectrum of DR1 in chloroform at the 2<sup>nd</sup> harmonic wavelength (solid curve).

A pronounced two-photon resonance with the charge-transfer (CT) excited state is clearly observed, and also the onset of a second resonance at higher energy is visible (most probably a two-photon resonance with the higher energy excited state also visible in the linear absorption spectrum), as well as a long-wavelength tail in the off-resonance region, converging towards the static value  $\beta_0$ . Note also that the two-photon resonance is significantly redshifted compared to the linear absorption band, in line with previous observations [17,19,27,30,32,39]. The highest  $\beta$  values are obtained in the most polar solvent acetonitrile, as can be expected for a NLO chromophore at the left hand side in the Bond Length Alternation (BLA) diagram [80,81]. Based on the three longest wavelength data points

and the undamped TLM, DR1 is found to have a static value  $\beta_{zzz,0}^{eff}$  of  $160 \times 10^{-30}$  esu in chloroform ( $\lambda_{eg} = 481$  nm), and  $107 \times 10^{-30}$  esu in pentafluorobenzonitrile ( $\lambda_{eg} = 498$  nm).

Calibration against the HRS signal of the pure solvent is applied over the entire wavelength range, using the calibration parameters from Table 2. The experimental error on the obtained  $\beta$  values (not including the systematic error on the reference standard value) is estimated to be about  $\pm 5\%$ . Due to the very poor photochemical stability of DR1 in chloroform at short excitation wavelengths, the measurements below 760 nm were performed in extra dry chloroform (Acros, 99.9 %, water < 50 ppm), and below 640 nm acetonitrile was used. We observed that upon short wavelength laser excitation in chloroform, a shoulder at the long-wavelength side of the CT absorption band of DR1 appeared, together with a red shift of this band and a decrease of its intensity. Such an unexplained redshift of the absorption maximum was also observed for a similar azobenzene derivative (DR13) in a Langmuir-Blodgett film after exposure to 514 nm laser light [82]. We found that this effect could not be reversed by illumination in this long wavelength shoulder by means of a dye laser. In acetonitrile however, only very limited decomposition was observed after exposure to 600 nm laser light, which was compensated for by stirring the solution. The  $\beta$  values of DR1 at 600 and 620 nm are estimated to have an experimental error of  $\pm 10\%$ . Fig. 6 clearly demonstrates that the present setup enables very accurate HRS measurements in the fundamental wavelength region of 600 to 1800 nm, revealing the detailed wavelength dependence of the molecular first hyperpolarizability  $\beta$  in both the resonant and the off-resonant region.

## Conclusions

In conclusion, a highly efficient setup for wavelength-dependent hyper-Rayleigh scattering (HRS) measurements has been developed, making use of a continuously tunable high repetition rate laser system with an optical parametric amplifier (OPA) and implementing single-photon sensitive parallel detection by means of an intensified CCD with thresholding scheme. Measurements can be performed over an extremely wide fundamental wavelength range (600 to 1800 nm) and thanks to the high detection sensitivity, reliable calibration against the pure solvent is reached over the entire spectral range. Moreover, the combination of efficient detection with high stability of the laser system yields an excellent S/N ratio and the (parallel) detection of a narrow spectral range around the second harmonic wavelength allows for a reliable elimination of background signals, MPF in particular. To be able to take into account the (limited)  $\beta$  dispersion of the pure solvent and to make sure that there are no significant vibrational resonance contributions near the IR absorption bands, an extensive series of  $\beta$  measurements was performed on eight different solvents relative to chloroform. It is found that, to a good approximation and over a wide spectral range, they all follow the simple undamped two-level model with a far UV resonance, providing extensive and accurate calibration data for future HRS measurements in these solvents. Two solvents (bromoform and pentafluorobenzonitrile) were identified as being particularly useful for HRS at the longest wavelengths, based on their IR transparency combined with the strength of their HRS signal. Finally, the qualities of the instrument are demonstrated by accurate tunable wavelength HRS measurements of the molecular first hyperpolarizability  $\beta$  for the well-known push-pull molecule Disperse Red 1.

## Acknowledgments

J. C. is a Postdoctoral Fellow of the Fund for Scientific Research of Flanders (FWO – Vlaanderen, Belgium). Financial support from FWO group projects G.0041.01 and G.0129.07 is gratefully acknowledged.